Avalanche Characteristics of $Al_xGa_{1-x}N$ Avalanche Photodiodes

Wesley Ooi Tat Lung, Cheang Pei Ling, You Ah Heng and Chan Yee Kit
Faculty of Engineering and Technology, Multimedia University, Jalan Ayer Keroh Lama, 75450 Melaka, Malaysia.
ahyou@mmu.edu.my

***Abstract*— AlGaN APDs are ultra-wide-bandgap semiconductor which has great potential, especially UV detection. In this work, Monte Carlo model has been developed to simulate the avalanche characteristics of thin $Al_xGa_{1-x}N$ APDs with random ionization path lengths incorporating dead space effect in a wide range of x value. Holes dominate the impact ionization at higher field for $Al_{0.3}Ga_{0.7}N$, whereas electrons dominate the impact ionization for $Al_{0.7}Ga_{0.3}N$. $Al_{0.3}Ga_{0.7}N$ also has higher electron and hole ionization coefficients compared to $Al_{0.7}Ga_{0.3}N$. Hole-initiated multiplication leads the mean multiplication gain for $Al_{0.3}Ga_{0.7}N$ APDs, while electron-initiated multiplication leads the mean multiplication gain for $Al_{0.7}Ga_{0.3}N$ APDs. The breakdown voltage and excess noise at fixed mean multiplication gain of 10 and 20 are then compared. The breakdown voltage increases as the Al content increases. The excess noise of hole-initiated multiplication is the lowest at $x \approx 0.4$ while excess noise of electron-initiated multiplication is lowest at $x = 0.7$. This shows that the ideal Al content is at $x \approx 0.4$ as the excess noise is low with manageable breakdown voltage as excess noise for hole-initiated multiplication decreases as x approaching 0.4.**

***Index Terms*— Aluminium Gallium Nitride (AlGaN); Avalanche Photodiodes; Excess Noise Factor; Impact Ionization; Multiplication Gain.**

I. INTRODUCTION

Gallium Nitride (GaN) is a material classified as a wide-bandgap semiconductor since it has a bandgap of 3.4 eV. Research on wide-bandgap semiconductor materials, particularly the GaN has been conducted as early as the 1980s, and it is still ongoing, especially on GaN avalanche photodiodes (APDs). The main principle of Avalanche Photodiode is the impact of ionization. In this case, when the energy (phonon) from a light source is received, the APD will amplify that energy until it is sufficient to be detected. GaN APDs have been developed since the mid-1970s, focusing on photon detection, optical communications and 3-D imaging [1, 2]. The potential for GaN APDs to be an excellent ultraviolet (UV) detector has the main factor that drives the research and development in this area [3]. UV detection is important for many applications such as chemical and biological sensing, applications in flame and missile plume detection, covert space-to-space communication and astronomical studies [4, 5]. The potential of GaN APDs as an UV detector enables GaN APDs to replace the current UV detectors such as photomultiplier tubes (PMTs) and thermal detector as PMTs have the disadvantage of being bulky, fragile and require a high power source, while thermal detector requires calibration in the UV range [3, 4, 5].

Furthermore, there are semiconductor materials, which have higher bandgap than GaN, known as ultra-wide-bandgap semiconductors. $Al_xGa_{1-x}N$, $(0 < x < 1)$ is an example of ultra-wide-bandgap semiconductor with bandgap ranging from 3.4 eV to 6.2 eV depending on the Al content. Ultra-wide-bandgap semiconductors have benefited many applications such as switching power conversion, RF electronics, UV optoelectronics, and quantum information [6, 7]. There are great interests on AlGaN APDs mainly due to the properties of having low dark current, high optical gain and high sensitivity [8]. In addition, with the Al content above 40 percent, AlGaN APDs has solar-blind properties, which make the AlGaN APDs a good candidate for UV detection as APDs without solar-blind properties require an additional filter to realize the solar-blindness [9, 10]. This enables AlGaN APDs to potentially replace narrow-bandgap semiconductor photodiodes, such as silicon based APDs as silicon based APDs require additional filtering that are quite costly [5, 9, 10].

While there are many research focused on optimizing the multiplication gain of AlGaN, not many works have been reported for AlGaN APDs with thin device at high electric field, including dead space effect, especially on $Al_{0.3}Ga_{0.7}N$ and $Al_{0.7}Ga_{0.3}N$ APDs. Besides, many of the literature work differ among each other, especially on the impact ionization coefficient [11, 12, 13] and multiplication gain [9, 14]. In this work, a Monte Carlo (MC) model is developed to simulate the impact ionization coefficients, mean multiplication gains and excess noise factors for both electron and hole with dead space effect for $Al_{0.3}Ga_{0.7}N$ and $Al_{0.7}Ga_{0.3}N$ APDs with the comparison on breakdown voltage and excess noise factor with our GaN and $Al_{0.45}Ga_{0.55}N$ APDs with thin multiplication width ranging from 0.1 µm to 0.3 µm. This work mainly focuses on simulating $Al_xGa_{1-x}N$ with a range of x values to determine the effect of increasing Al content on the breakdown voltage, multiplication gain and excess noise.

II. IMPACT IONIZATION COEFFICIENTS

Impact ionization is a process that is able to amplify weak photocurrent or light until it is sufficient to be detected by an electronic circuit. This process occurs between the conduction and valence band of an APD and is initiated by electron or hole. When an APD absorbs photon from the light, an electron-hole pair is created. After the electron (hole) absorbs enough energy, the electron (hole) from the conduction (valence) band will excite an electron (hole) from the valence (conduction) band to the conduction (valence) band. In a condition when the carrier receives enough energy

that is, the amount of energy is higher than the APD bandgap [15, 16], and collides with the lattice atom, a second electron-hole pair will be created from impact ionization. The carriers, the original and the newly created are accelerated due to the influence of the electric field and impact ionizes, subsequently generates additional electron-hole pairs [16]. This process will occur repeatedly until all the carriers leave the multiplication region. The mean multiplication gain and excess noise of the APD is largely dependent on the impact ionization, where higher impact ionization coefficient generally is translated to higher gain and lower breakdown voltage.

Impact ionization coefficients are the number of electron-hole pairs generated per unit distance traveled by a solitary carrier between two collisions. The coefficients are evaluated based on the number of carriers scattered from the impact ionization. The coefficients are separated into electron (α) and hole (β) and are computed based on:

$$\alpha = \left[\sum_{i=1}^{n_e} l_{ei} \Big/ n_e\right]^{-1} \ cm^{-1} \quad (1)$$

$$\beta = \left[\sum_{i=1}^{n_h} l_{hi} \Big/ n_h\right]^{-1} \ cm^{-1} \quad (2)$$

where: n_e = Number of electrons scattered
n_h = Number of holes scattered
l_{ei} = Travelling distance of electron
l_{hi} = Travelling distance of hole

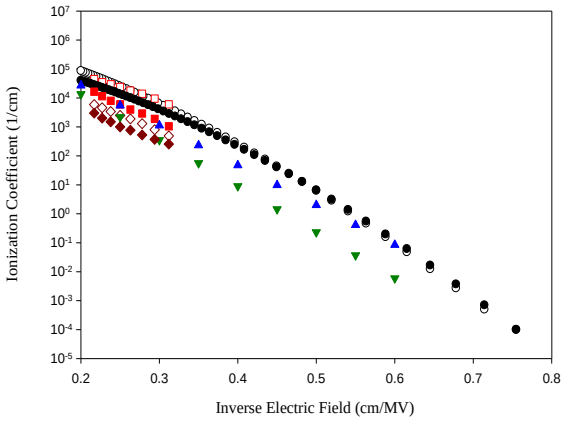

Figure 1: Electron ionization coefficient, α (filled black circle) and hole ionization coefficient, β (empty black circle) of $Al_{0.3}Ga_{0.7}N$ from this work compared to Bulutay [12] ($Al_{0.2}Ga_{0.8}N$ α: blue upright triangle; $Al_{0.4}Ga_{0.6}N$ α: green inverted triangle), and Bellotti [13] $Al_{0.2}Ga_{0.8}N$ (α: filled red square, β: empty red square) and $Al_{0.4}Ga_{0.6}N$ (α: filled brown diamond, β: empty brown diamond)

Figure 1 shows the impact ionization coefficients of $Al_{0.3}Ga_{0.7}N$ of our work compared with the literature. Due to the difficulty in obtaining impact ionization coefficients of $Al_{0.3}Ga_{0.7}N$ from literature, it is compared with the two closest Al content, $Al_{0.2}Ga_{0.8}N$ and $Al_{0.4}Ga_{0.6}N$. The electron and hole ionization coefficients for $Al_{0.3}Ga_{0.7}N$ in our work is a slightly higher than that of Bulutay [12] and Bellotti *et al.* [13], where the impact ionization coefficient from our work is closer to the literature $Al_{0.2}Ga_{0.8}N$ instead of in between x = 0.2 and x = 0.4. However, the result is still close, and the differences can be attributed to the differences in the material parameters and the model used. In addition, hole dominates the impact ionization especially at a higher field. This condition agrees with the literature review where hole will dominate the impact ionization at high electric field [11, 12, 13, 17].

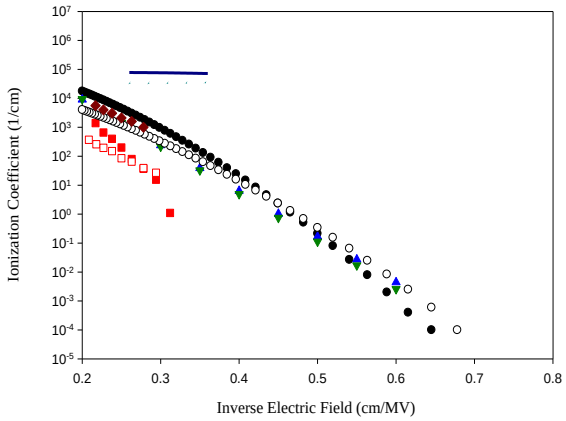

Figure 2: Electron ionization coefficient, α (filled black circle) and hole ionization coefficient, β (empty black circle) of $Al_{0.7}Ga_{0.3}N$ from this work compared to Bulutay [12] ($Al_{0.6}Ga_{0.4}N$ α: green inverted triangle; $Al_{0.8}Ga_{0.4}N$ α: blue upright triangle), Bellotti *et al.* [13] $Al_{0.6}Ga_{0.4}N$ (α: filled red square, β: empty red square), $Al_{0.8}Ga_{0.2}N$ (α: filled brown diamond) and Yan *et al.* [18] $Al_{0.6}Ga_{0.4}N$ (α: Blue solid line, β: cyan dotted line)

Table 1
Parameters for Impact Ionization Coefficients for $Al_xGa_{1-x}N$

x	Carrier	$A_{e/h}$ (cm^{-1})	$B_{e/h}$ (V/cm)	γ
0	α	7.32×10^7	7.16×10^8	1.90
	β	3.48×10^7	6.56×10^8	1.65
0.3	α	4.07×10^7	8.21×10^8	1.70
	β	1.51×10^8	9.64×10^8	1.60
0.45	α	1.66×10^7	8.51×10^8	1.75
	β	8.01×10^7	1.02×10^9	1.65
0.7	α	3.05×10^7	9.10×10^8	1.75
	β	5.68×10^6	9.03×10^8	1.65

Figure 2 shows the impact ionization coefficients of $Al_{0.7}Ga_{0.3}N$ of our work compared with the literature. Opposing $Al_{0.3}Ga_{0.7}N$ of our work, the $Al_{0.7}Ga_{0.3}N$ has electron that dominates the impact ionization at high electric field. This is consistent with the literature where electron will dominate the impact ionization when $x > 0.5$ [13, 18]. This is due to the alloy scattering that is increasing as x approaches 0.5, where the maximum alloy scattering occurs at $x \approx 0.5$ [13]. As x = 0.7 is near the material properties of AlN, alloy scattering is reduced, and therefore electron impact ionization is unlikely to be hindered by the alloy scattering. However, the hole ionization coefficient of AlN itself is extremely low [13], as the x value approaches one, which is AlN, the hole ionization coefficient will decrease. Both electron and hole ionization coefficients of $Al_{0.7}Ga_{0.3}N$ is lower compared to $Al_{0.3}Ga_{0.7}N$. Our work is closed to Bulutay [12] but an order of magnitude higher than Bellotti *et al.* and is lower than Yan *et al.* [18] experimental work. It is explained in Tut *et al.* [11] work that the lattice defect from the AlGaN layer in experiments will cause discrepancy. The difference between our work and literature is due to the differences in the material

parameters and simulation model used during simulation. The electric field dependent impact ionization coefficient expressions obtained in our work are deduced and presented as Equations (3) and (4), where the parameters are listed in Table 1 and the additional parameters for GaN and $Al_{0.45}Ga_{0.55}N$ are from our previous work [19].

$$\alpha = A_e \, exp\left[-\left(\frac{B_e}{E}\right)^{\gamma}\right] \, cm^{-1} \tag{3}$$

$$\beta = A_h \exp\left[-\left(\frac{B_h}{E}\right)^{\gamma}\right] \, cm^{-1} \tag{4}$$

III. Multiplication Gain and Excess

By injecting electron or hole into the multiplication region of an APD, the multiplication process is initiated [20]. The carrier will then gain energy when drifted under uniform electric field, generating large amounts of electron-hole pairs. The electron-hole pairs will be generated until all the carriers leave the multiplication region.

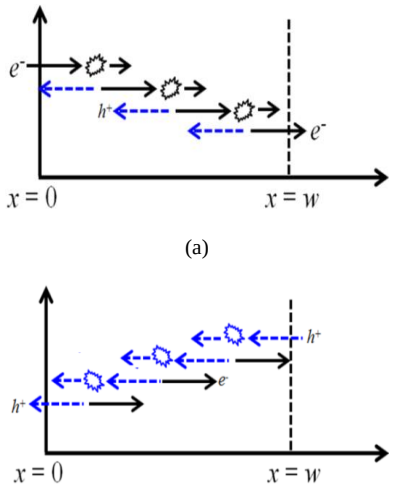

Figure 3: (a) Electron-initiated impact ionization, and (b) Hole-initiated impact ionization

Figures 3(a) and (b) show the schematics of electron-initiated and hole-initiated impact ionization respectively. For electron-initiated multiplication, electron is injected at $x = 0$, where the electron will drift through a random distance (l_e). This random distance include dead space, where dead space is the distance required for the electron to acquire enough energy to impact ionize [21], and thus the electron cannot impact ionize within the dead space distance. The random path length is calculated by [21, 22, 23]

$$l_e = d_e - \frac{\ln r}{\alpha} \tag{5}$$

where: d_e = Dead space region for electron
r = Random number from 0 to 1

For hole-initiated multiplication, hole is injected at the opposite end, where $x = w$, w is the width of the multiplication region, and the hole will drift through the negative x-direction with a random path length (l_h) including the dead space (d_h). The random path length for hole is calculated by:

$$l_h = d_h - \frac{\ln r}{\beta} \tag{6}$$

The mean multiplication gain ($\langle M \rangle$) and the excess noise factor (F) is computed by the total number of trials considered by the simulation generated by a specific random number, as shown in Equations (7) and (8).

$$\langle M \rangle = \frac{1}{n}\sum_{i=1}^{n} M_i \tag{7}$$

$$F = \frac{\sum_{i=1}^{n} M_i^2}{n\langle M \rangle^2} \tag{8}$$

Figure 4 shows the electron- and hole-initiated multiplication gain with dead space effect as a function of reversed biased voltage with differing multiplication widths, w of 0.1 μm, 0.14 μm, 0.18 μm, 0.2 μm and 0.26 μm of $Al_{0.3}Ga_{0.7}N$ APDs. In our simulation, hole is leading the multiplication gain at all multiplication widths. This is consistent with our results where hole dominates the impact ionization for $Al_{0.3}Ga_{0.7}N$, as shown in Figure 1. Due to the limited researches on the gain of $Al_{0.3}Ga_{0.7}N$ APDs, the results of $Al_{0.2}Ga_{0.8}N$ and $Al_{0.15}Ga_{0.85}N$ APDs are also included for comparison as the Al content is quite close. $Al_{0.4}Ga_{0.6}N$ APD is not included in the comparison in this figure as impact ionization coefficient rapidly decreases as the Al content approaches 0.4 to 0.5 [13], which comparatively will have much higher breakdown voltage. Our results are consistent with Tang *et al.* [24] N-face experiment, whereas differs from Tang's Ga-face experiment differs. Our results are reasonably consistent to other literature results besides Yao *et al.* [25], which differs from the normal trend.

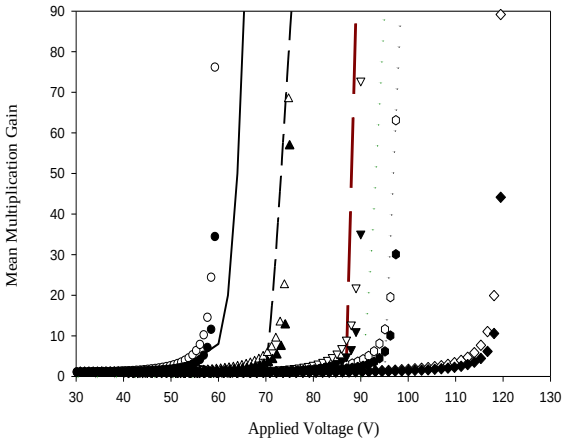

Figure 4: Electron (filled symbols) and hole (empty symbols) -initiated multiplication gain with w = 0.1 μm (circle), 0.14 μm (upright triangle), 0.18 μm (down-pointing triangle), 0.2 μm (hexagon) and 0.26 μm (diamond) of $Al_{0.3}Ga_{0.7}N$ APDs from this work compared with Tang *et al.* [24] $Al_{0.3}Ga_{0.7}N$ APDs (0.14 μm, Ga face – black dotted line; N face – black dashed line), Dong *et al.* [9] $Al_{0.15}Ga_{0.85}N$ APDs (0.18 μm, red dashed line), Yao *et al.* [25] $Al_{0.15}Ga_{0.85}N$ APDs (0.18 μm, black solid line) and Cai *et al.* [26] $Al_{0.2}Ga_{0.8}N$ APDs (0.18 μm, green dotted line)

Figure 5 shows our simulation for $Al_{0.7}Ga_{0.3}N$ APDs with dead space effect with w of 0.1 μm, 0.18 μm, 0.2 μm, 0.26 μm and 0.3 μm. In this simulation, electron is leading the multiplication gain with considerable margin compared to hole at all w. This agrees with the research from literature [13,

27], where electron will dominate the impact ionization for $x > 0.5$ and electron will lead the multiplication gain for $Al_{0.7}Ga_{0.3}N$ APDs. As there is a limited research on the gain of $Al_{0.7}Ga_{0.3}N$ APDs, the closest Al content of $Al_{0.6}Ga_{0.4}N$ is used for comparison instead. Our result for 0.1 μm is quite similar to Bellotti *et al.* [27] $Al_{0.6}Ga_{0.4}N$ APDs on $w = 0.1$ μm, fairly closed to $w = 0.2$ μm and differs from $w = 0.3$ μm. This can be attributed on the difference between the simulation model used and the different Al content, where our work deals with $x = 0.7$ and the literature deals with $x = 0.6$. For all Al content, the breakdown voltage increases as w becomes wider. This will allow the carriers to have higher multiplication gain as there are more chances for impact ionization to occur, but usually at the cost of higher excess noise.

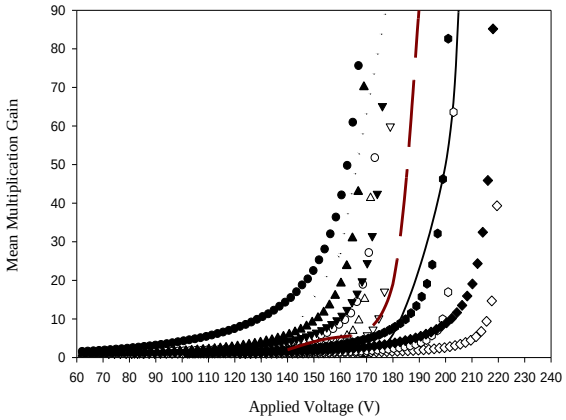

Figure 5: Electron (filled symbols) and hole (empty symbols) -initiated multiplication gain with $w = 0.1$ μm (circle), 0.18 μm (upright triangle), 0.2 μm (down-pointing triangle), 0.26 μm (hexagon) and 0.3 μm (diamond) of $Al_{0.7}Ga_{0.3}N$ APDs from this work compared with Bellotti *et al.* [27] $Al_{0.6}Ga_{0.4}N$ APDs (0.1 μm, black dotted line; 0.2 μm, red dashed line; 0.3 μm black solid line)

Figure 6 shows the excess noise factor of electron- and hole-initiated multiplication in $Al_{0.3}Ga_{0.7}N$ APDs respectively with w of 0.1 μm, 0.14 μm, 0.18 μm, 0.2 μm and 0.26 μm, including dead space effect. The excess noise factor for hole-initiated multiplication is much lesser than that of electron. The electron-initiated multiplication has high excess noise due to the higher hole ionization coefficient compared to that of electron, which indicates large amount of feedback holes in the multiplication region [16, 28]. In addition, the excess noise factor of electron-initiated multiplication is increasing near linearly with multiplication gain and has almost the same gradient at all w, indicating high noise at all w for electron-initiated multiplication from the $Al_{0.3}Ga_{0.7}N$ APDs. The excess noise for hole-initiated multiplication however diverges with increasing w as multiplication gain increases. As w increases, the excess noise factor will slightly increase due to higher chances of impact ionization to happen.

Figure 7 shows the excess noise factor of electron- and hole-initiated multiplication of $Al_{0.7}Ga_{0.3}N$ APDs with differing w of 0.1 μm, 0.18 μm, 0.2 μm, 0.26 μm and 0.3 μm. Differing from $Al_{0.3}Ga_{0.7}N$ APDs, the excess noise for electron-initiated multiplication is much lower for $Al_{0.7}Ga_{0.3}N$ APD compared to hole-initiated. This is mainly due to the fact that $Al_{0.7}Ga_{0.3}N$ APD has higher electron ionization coefficient than that of the hole, which indicates less feedback ionizations by holes in the multiplication region. Opposing $Al_{0.3}Ga_{0.7}N$ APDs, the excess noise for electron-initiated diverges with increasing w, where the excess noise increases slightly as w increases. The excess noise factor of hole-initiated multiplication, on the other hand it has almost constant average gradient with increasing w and has more than threefold the excess noise compared to multiplication gain.

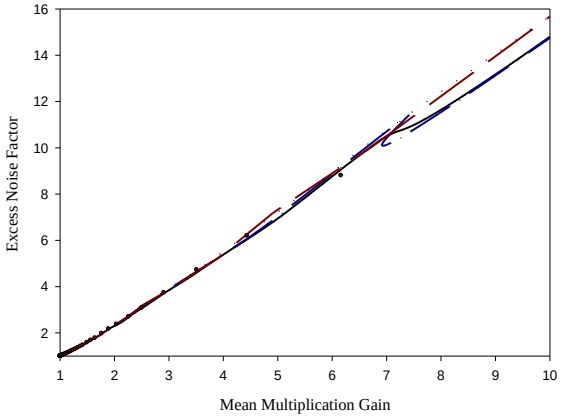

(a)

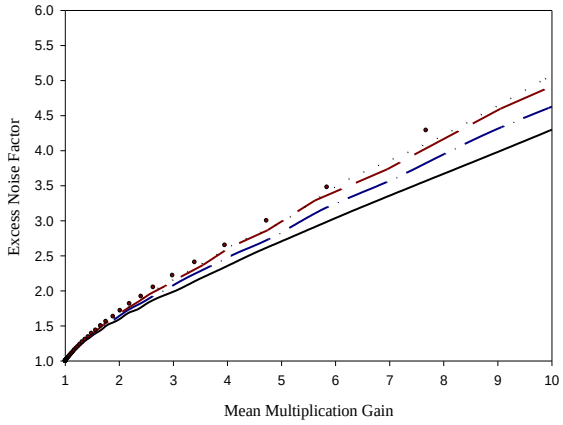

(b)

Figure 6: Excess noise factor of (a) electron- and (b) hole-initiated multiplication with $w = 0.1$ µm (black line), 0.14 µm (blue dash-dot-dash line), 0.18 µm (red dashed line), 0.2 µm (black dotted line) and 0.26 µm (red dots) of $Al_{0.3}Ga_{0.7}N$ APDs

Figure 8 represents the comparison of breakdown voltage between different Al content ($0 \leq x \leq 0.7$) where $x = 0$ represents GaN APDs with multiplication gain of 10 and 20 from our work [19]. It is noticed that the trend of the breakdown voltage is nearly similar even as the gain increased from 10 to 20. From the simulation, the breakdown voltage of all Al content increases when w becomes wider. For the hole-initiated impact ionization, the breakdown voltage increases slightly when the Al content is increased from 0 to 30%. After $x \approx 0.4$, the breakdown voltage increased sharply where $Al_{0.7}Ga_{0.3}N$ APDs has extremely high breakdown voltage. The hole-initiated breakdown voltage for $Al_{0.7}Ga_{0.3}N$ APDs at $w = 0.1$ µm is extremely high to the point it reaches the electron-initiated breakdown voltage of $Al_{0.7}Ga_{0.3}N$ APDs at $w = 0.2$ µm for both multiplication gain of 10 and 20. The high breakdown voltage of $Al_{0.7}Ga_{0.3}N$ APD makes it inefficient to be used for multiplication layer in real life application as the layer has to be grown in such a quality that it can support extremely high electric field [27]. Besides, the high breakdown voltage will produce high heat,

which results in increased thermal noise [16]. It can be deduced that from GaN APDs until $Al_{0.4}Ga_{0.6}N$ APDs in Al content is the most efficient to be used as multiplication layer as the breakdown voltage is relatively low. $Al_{0.45}Ga_{0.55}N$ APDs is fairly higher than $Al_{0.4}Ga_{0.6}N$ APDs in breakdown voltage of approximately 10 volts based on approximation of the graph, but it is still within the reasonable range; thus, there are quite a number of researches on $Al_{0.45}Ga_{0.55}N$ APDs. Nevertheless, both $Al_{0.4}Ga_{0.6}N$ and $Al_{0.45}Ga_{0.55}N$ APDs exhibit solar blind properties [9, 26], which make them a popular candidate for UV detection.

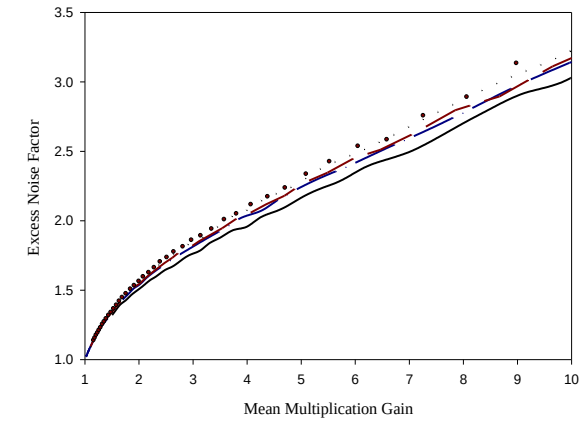

(a)

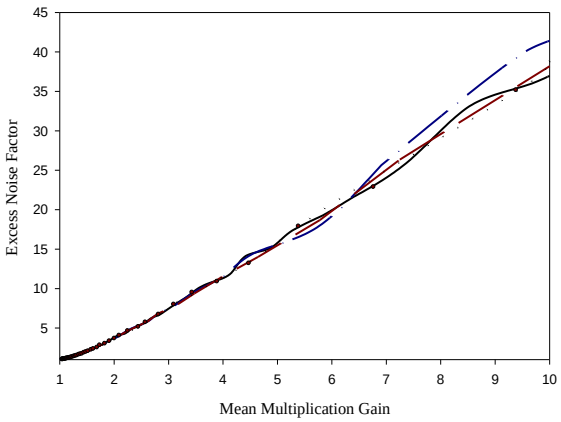

(b)

Figure 7: Excess noise factor of (a) electron- and (b) hole-initiated multiplication with $w = 0.1$ μm (black line), 0.18 μm (blue dash-dot-dash line), 0.2 μm (red dashed line), 0.26 μm (black dotted line) and 0.3 μm (red dots) of $Al_{0.7}Ga_{0.3}N$ APDs

Figure 9 shows our work comparison of excess noise factor between different Al content ($0 \leq x \leq 0.7$) where $x = 0$ represents GaN APDs with multiplication gain of 10 and 20. The trend for excess noise factor is nearly similar for multiplication gain of 10 and 20. For $w = 0.1$ μm and $w = 0.2$ μm, the hole-initiated impact ionization has the lowest excess noise at $x \approx 0.4$, whereas electron-initiated impact ionization has the highest excess noise at $x \approx 0.4$. The low excess noise of hole-initiated impact ionization combined with the solar-blind properties of $Al_{0.4}Ga_{0.6}N$ and $Al_{0.45}Ga_{0.55}N$ APDs makes them an attractive choice for heterojunction AlGaN APD by introducing a layer of different material or AlGaN with different Al percentage to suppress the electron ionization [29, 30]. This will trap the feedback electrons, resulting in an APD that has low excess noise. The highest excess noise for hole-initiated multiplication and the lowest excess noise for electron-initiated multiplication are both from $Al_{0.7}Ga_{0.3}N$ APDs. The low excess noise factor of electron-initiated multiplication for $Al_{0.7}Ga_{0.3}N$ APDs would suggest $Al_{0.7}Ga_{0.3}N$ APD a good candidate for UV detection since it also has solar blind properties. However, this is hindered by the high breakdown voltage of $Al_{0.7}Ga_{0.3}N$ APD, making it unsuitable to be used in the multiplication layer of an APD with current device fabrication technology [27].

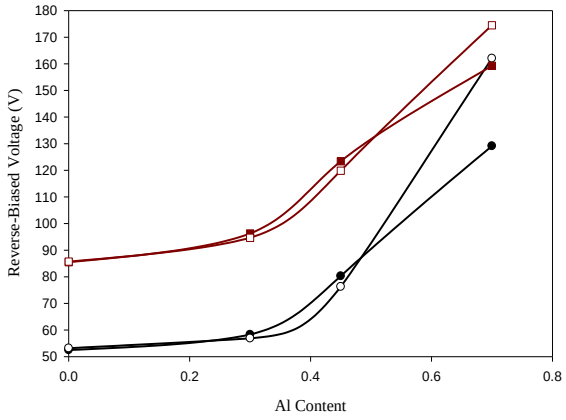

(a)

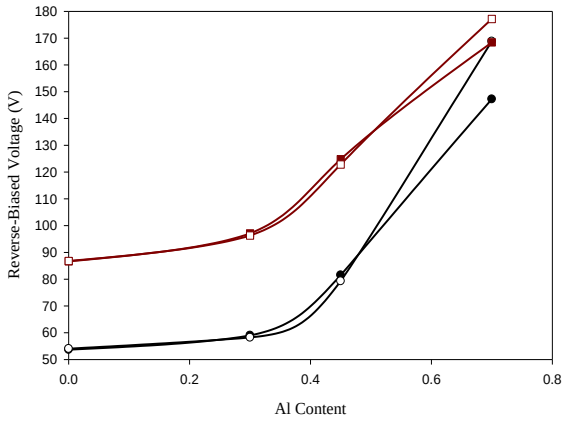

(b)

Figure 8: Comparison of breakdown voltage between different Al content with multiplication gain of (a) 10 and (b) 20. The black lines represent $w = 0.1$ μm (Electron: filled black circle, hole: empty black circle) and red lines represent $w = 0.2$ μm (Electron: filled red square, hole: empty red square)

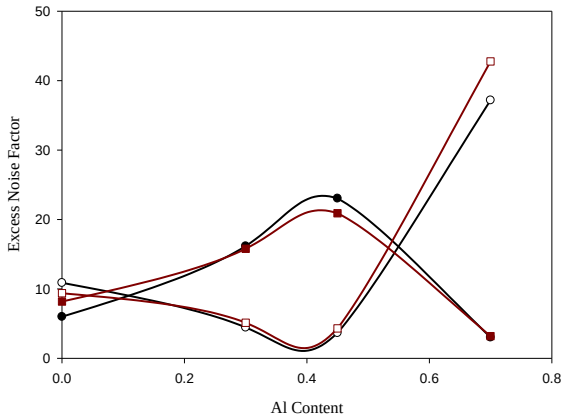

(a)

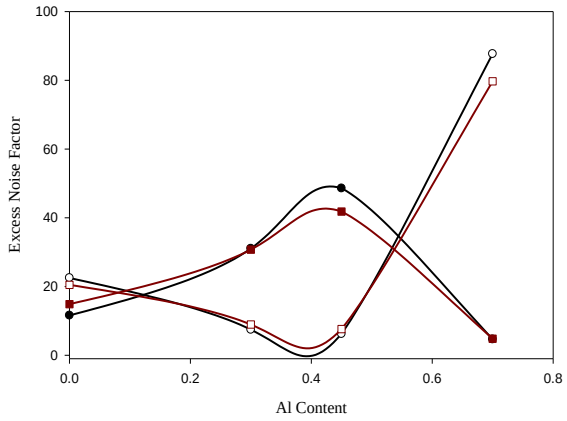

(b)

Figure 9: Comparison of excess noise factor between different Al content with multiplication gain of (a) 10 and (b) 20. The black lines represent w = 0.1 μm (Electron: filled black circle, hole: empty black circle) and red lines represent w = 0.2 μm (Electron: filled red square, hole: empty red square)

IV. CONCLUSION

A Monte Carlo model is developed to simulate the avalanche characteristics of $Al_xGa_{1-x}N$ ($0 < x \leq 0.7$) APD. Hole dominates the impact ionization for $Al_{0.3}Ga_{0.7}N$ whereas for $Al_{0.7}Ga_{0.3}N$, electron dominates the impact ionization. Hole-initiated multiplication gives a higher gain and lower excess noise compared to electron-initiated multiplication for $Al_{0.3}Ga_{0.7}N$ APDs at all multiplication widths, whereas for $Al_{0.7}Ga_{0.3}N$ APDs the opposite happens; where electron-initiated multiplication has a higher gain and lower excess noise. The breakdown voltage increases with increasing Al content, resulting in high breakdown voltage for $Al_{0.7}Ga_{0.3}N$ APDs and is inefficient to be used as multiplication layer of an APD. The lowest excess noise for electron-initiated and hole-initiated multiplication occurs in $Al_{0.7}Ga_{0.3}N$ and $Al_{0.4}Ga_{0.6}N$ APDs respectively. The low excess noise of hole-initiated multiplication for $Al_{0.4}Ga_{0.6}N$ and $Al_{0.45}Ga_{0.55}N$ APDs is useful in heterojunction APDs, where the electrons feedback can be suppressed. $Al_{0.7}Ga_{0.3}N$ APDs has low excess noise of electron-initiated multiplication, but due to the high breakdown voltage combined with the limitation of current device fabrication technology, there will be difficulty in introducing $Al_{0.7}Ga_{0.3}N$ APD as multiplication layer in a heterojunction APD. The low excess noise factor, innate solar-blind properties combined with the manageable breakdown voltage of $Al_{0.45}Ga_{0.55}N$ APDs made it the most excellent candidate out of all the simulated APDs to be used as the multiplication layer in a heterojunction APD.

REFERENCES

[1] J. C. Campbell, "Recent Advances in Telecommunications Avalanche Photodiodes", *Journal of Lightwave Technology*, vol. 25, no. 1, pp. 109–121, 2007.

[2] J. C. Campbell, "Recent Advances in Avalanche Photodiodes", *Journal of Lightwave Technology*, vol. 34, no. 2, pp. 278–285, 2016.

[3] H. You, Z. Shao, Y. Wang, L. Hu, D. Chen, H. Lu, R. Zhang and Y. Zheng, "Fine Control of the Electric Field Distribution in the Heterostructure Multiplication Region of AlGaN Avalanche Photodiodes", *IEEE Photonics Journal*, vol. 9, no. 3, pp. 1–7, 2017.

[4] J. Bulmer, P. Suvarna, J. Leathersich, J. Marini, I. Mahaboob, N. Newman and F. S. Shahedipour-Sandvik, "Visible-Blind APD Heterostructure Design With Superior Field Confinement and Low Operating Voltage", *IEEE Photonics Technology Letters*, vol. 28, no. 1, pp. 39–42, 2016.

[5] E. Monroy, F. Omnès and F. Calle, "Wide-bandgap semiconductor ultraviolet photodetectors", *Semiconductor Science and Technology*, vol. 2, no. 4, pp. 33, 2003.

[6] J. Y. Tsao *et al.*, "Ultrawide-bandgap semiconductors: Research opportunities and challenges", *Advanced Electron. Materials*, pp. 1600501, 2017.

[7] R. J. Kaplar, A. A. Allerman, A. M. Armstrong, M. H. Crawford, J. R. Dickerson, A. J. Fischer, A. G. Baca and E. A. Douglas, "Review-Ultra-wide-bandgap AlGaN power electronic devices", *ECS Journal of Solid State Science and Technology*, vol. 6, no. 2, pp. Q3061–Q3066, 2017.

[8] Z. Huang, J. Li, W. Zhang and H. Jiang, "AlGaN solar-blind avalanche photodiodes with enhanced multiplication gain using back-illuminated structure", *Applied Physics Express*, vol. 6, no. 5, pp. 054101, 2013.

[9] K. Dong, D. Chen, B. Jin, X. Jiang and J. Shi, "$Al_{0.4}Ga_{0.6}N/Al_{0.15}Ga_{0.85}N$ Seperate Absorption and Multiplication Solar-Blind Avalanche Photodiodes with a One-Dimensional Photonic Crystal Filter", *IEEE Photonics Journal*, vol. 8, no. 4, pp. 1–7, 2016.

[10] R.D. Dupuis, J. Ryou, D. Yoo, J. B. Limb, Y. Zhang, S. Shen and D. Yoder, "High-performance GaN and $Al_xGa_{1-x}N$ ultraviolet avalanche photodiodes grown by MOCVD on bulk III-N substrates", *Proceedings of SPIE*, vol. 6739, pp. 67391B, 2007.

[11] T. Tut, M. Gokkavas, B. Butun, S. Butun, E. Ulker and E. Ozbay, "Experimental evaluation of impact ionization coefficients in $Al_xGa_{1-x}N$ based avalanche photodiodes", *Applied Physics Letters*, vol. 89, pp. 183524, 2006.

[12] C. Bulutay, "Electron initiated impact ionization in AlGaN alloys", *Institute of Physic Publishing, Semiconductor Science and Technology*, vol. 17, no. 10, pp. 59-62, 2002.

[13] E. Bellotti and F. Bertazzi, "A numerical study of carrier impact ionization in $Al_xGa_{1-x}N$", *Journal of Applied Physics*, vol. 111, pp. 103711, 2012.

[14] Z. G. Shao, D. J. Chen, H. Lu, R. Zhang, D. P. Cao, W. J. Luo, Y. D. Zheng, L. Li and Z. H. Li, "High-Gain AlGaN Solar-Blind Avalanche Photodiodes", *IEEE Electron Device Letters*, vol. 35, no. 3, pp. 372–374, 2014.

[15] S. M. Sze and K. K. Ng, "Physics and Properties of Semiconductors-A Review", *In: Physics of Semiconductor Devices*, John Wiley & Sons, Inc., pp. 82, 2006.

[16] B. E. A. Saleh and M. C. Teich, "Semiconductor Photon Detectors", *In: Fundamentals of Photonics*, John Wiley & Sons, Inc., pp. 666–667, 1991.

[17] M. Hou, Z. Qin, C. He, L. Wei, F. Xu, X. Wang and B. Shen, "Study on AlGaN p-i-n-i-n solar-blind avalanche photodiodes with $Al_{0.45}Ga_{0.55}N$ multiplication layer", *Electronic Materials Letters*, vol. 11, no. 6, pp. 1053-1058, 2015.

[18] H. Yan, C. Liu, H. Wang, Z. Zhang, M. Chen and H. Jiang, "Avalanche Multiplication in Schottky-type AlGaN Photodiode with High Al-composition", *2018 Asia Communications and Photonics Conference (ACP)* [Hangzhou, China: IEEE, 2018].

[19] T. L. Wesley Ooi, P. L. Cheang, A. H. You, Y. K. Chan, "Mean Multiplication Gain & Excess Noise Factor of GaN and $Al_{0.45}Ga_{0.55}N$ Avalanche Photodiodes", *The European Physical Journal Applied Physics*, vol. 92, no. 1, pp. 10301, 2020.

[20] P. Yuan, K. A. Anselm, C. Hu, H. Nie, C. Lenox, A. L. Holmes, B. G. Streetman, J. C. Campbell and R. J. McIntyre, "A new look at impact ionization-Part II: Gain and noise in short avalanche photodiodes", *IEEE Transactions on Electron Devices*, vol. 46, no. 8, pp. 1632–1639, 1999.

[21] M. M. Hayat, W. L. Sargeant and B. E. A. Saleh, "Effect of dead space on gain and noise in Si and GaAs avalanche photodiodes", *IEEE Journal of Quantum Electronics*, vol. 28, no. 5, pp. 1360–1365, 1992.

[22] Y. Okuto and C. R. Crowell, "Threshold energy effect on avalanche breakdown voltage in semiconductor junctions", *Solid-State Electronics*, vol. 18, no. 2, pp. 161–168, 1975.

[23] S. A. Plimmer, J. P. R. David, D. S. Ong and K. F. Li, "A simple model for avalanche multiplication including deadspace effects", *IEEE Transactions on Electron Devices*, vol. 46, no. 4, pp. 769–775, 1999.

[24] Y. Tang, Q. Cai, L. Yang, K. Dong, D. Chen, H. Lu, R. Zhang and Y. Zheng, "High-Gain N-Face AlGaN Solar-Blind Avalanche Photodiodes Using a Heterostructure as Separate Absorption and Multiplication Regions", *Chinese Physics Letters*, vol. 34, no. 1, pp. 018502, 2017.

[25] C. Yao, X. Ye, R. Sun, G. Yang, J. Wang, Y. Lu, P. Yan, J. Cao and S. Gao, "High-performance AlGaN-based solar-blind avalanche photodiodes with dual-periodic III–nitride distributed Bragg reflectors", *Applied Physics Express*, vol. 10, no. 3, pp. 034302, 2017.

[26] Q. Cai, M. Ge, J. Xue, L. Hu, D. Chen, H. Lu, R. Zhang and Y. Zheng, "An Improved Design for Solar-Blind AlGaN Avalanche Photodiodes", *IEEE Photonics Journal*, vol. 9, no. 4, pp. 1–7, 2017.

[27] E. Bellotti and F. Bertazzi, "Numerical simulation of deep-UV avalanche photodetectors", *Physics and Simulation of Optoelectronic Devices XXII*, vol. 8980, pp. 89800R, 2014.

[28] G. M. Williams, M. Compton, D. A. Ramirez, M. M. Hayat and A. S. Huntington, "Multi-Gain-Stage InGaAs Avalanche Photodiode with Enhanced Gain and Reduced Excess Noise", *IEEE Journal of the Electron Devices Society*, vol. 1, no. 2, pp. 54–65, 2013.

[29] O. Kwon, M. M. Hayat, S. Wang, J. C. Campbell, A. Holmes, Y. Pan, B. E. A. Saleh and M. C. Teich, "Optimal Excess Noise Reduction in Thin Heterojunction $Al_{0.6}Ga_{0.4}As$–GaAs Avalanche Photodiodes", *IEEE Journal of Quantum Electronics*, vol. 39, no. 10, pp. 1287 – 1296, 2003.

[30] Z. Shao, X. Yang, H. You, D. Chen, H. Lu, R. Zhang, Y. Zheng and K. Dong, "Ionization-Enhanced AlGaN Heterostructure Avalanche Photodiodes", *IEEE Electron Device Letters*, vol. 38, no. 4, pp. 485–488, 2017.